

## 18 Spectroscopy 3: magnetic resonance

### Solutions to exercises

#### Discussion questions

---

- E18.1(b)** Before the application of a pulse the magnetization vector,  $M$ , points along the direction of the static external magnetic field  $B_0$ . There are more  $\alpha$  spins than  $\beta$  spins. When we apply a rotating magnetic field  $B_1$  at right angles to the static field, the magnetization vector as seen in the rotating frame begins to precess about the  $B_1$  field with angular frequency  $\omega_1 = \gamma B_1$ . The angle through which  $M$  rotates is  $\theta = \gamma B_1 t$ , where  $t$  is the time for which the  $B_1$  pulse is applied. When  $t = \pi/2\gamma B_1$ ,  $\theta = \pi/2 = 90^\circ$ , and  $M$  has rotated into the  $xy$  plane. Now there are equal numbers of  $\alpha$  and  $\beta$  spins. A  $180^\circ$  pulse applied for a time  $\pi/\gamma B_1$ , rotates  $M$  antiparallel to the static field. Now there are more  $\beta$  spins than  $\alpha$  spins. A population inversion has occurred.
- E18.2(b)** The basic COSY experiment uses the simplest of all two-dimensional pulse sequences: a single  $90^\circ$  pulse to excite the spins at the end of the preparation period, and a mixing period containing just a second  $90^\circ$  pulse (see Fig. 18.44 of the text).

The key to the COSY technique is the effect of the second  $90^\circ$  pulse, which can be illustrated by consideration of the four energy levels of an AX system (as shown in Fig. 18.12). At thermal equilibrium, the population of the  $\alpha A \alpha X$  level is the greatest, and that of  $\beta A \beta X$  level is the smallest; the other two levels have the same energy and an intermediate population. After the first  $90^\circ$  pulse, the spins are no longer at thermal equilibrium. If a second  $90^\circ$  pulse is applied at a time  $t_1$  that is short compared to the spin-lattice relaxation time  $T_1$  the extra input of energy causes further changes in the populations of the four states. The changes in populations will depend on how far the individual magnetizations have precessed during the evolution period.

For simplicity, let us consider a COSY experiment in which the second  $90^\circ$  pulse is split into two selective pulses, one applied to X and one to A. Depending on the evolution time  $t_1$ , the  $90^\circ$  pulse that excites X may leave the population differences across each of the two X transitions unchanged, inverted, or somewhere in between. Consider the extreme case in which one population difference is inverted and the other unchanged (Fig. 18.45). The  $90^\circ$  pulse that excites A will now generate an FID in which one of the two A transitions has increased in intensity, and the other has decreased. The overall effect is that precession of the X spins during the evolution period determines the amplitudes of the signals from the A spins obtained during the detection period. As the evolution time  $t_1$  is increased, the intensities of the signals from A spins oscillate at rates determined by the frequencies of the two X transitions.

This transfer of information between spins is at the heart of two-dimensional NMR spectroscopy and leads to the correlation of different signals in a spectrum. In this case, information transfer tells us that there is a scalar coupling between A and X. If we conduct a series of experiments in which  $t_1$  is incremented, Fourier transformation of the FIDs on  $t_2$  yields a set of spectra  $I(\nu_1, \nu_2)$  in which the A signal amplitudes oscillate as a function of  $t_1$ . A second Fourier transformation, this time on  $t_1$ , converts these oscillations into a two-dimensional spectrum  $I(\nu_1, \nu_2)$ . The signals are spread out in  $\nu_1$  according to their precession frequencies during the detection period. Thus, if we apply the COSY pulse sequence to our AX spin system (Fig. 18.44), the result is a two-dimensional spectrum that contains four groups of signals centred on the two chemical shifts in  $\nu_1$  and  $\nu_2$ . Each group will show fine structure, consisting of a block of four signals separated by  $J_{AX}$ . The diagonal peaks are signals centred on  $(\delta_A \delta_A)$  and  $(\delta_X \delta_X)$  and lie along the diagonal  $\nu_1 = \nu_2$ . They arise from signals that did not change chemical shift between  $t_1$  and  $t_2$ . The cross peaks (or *off-diagonal peaks*) are signals centred on  $(\delta_A \delta_X)$  and  $(\delta_X \delta_A)$  and owe their existence to the coupling between A and X.

Consequently, cross peaks in COSY spectra allow us to map the couplings between spins and to trace out the bonding network in complex molecules. Figure 18.46 shows a simple example of a proton COSY spectrum of 1-nitropropane.

- E18.3(b)** The molecular orbital occupied by the unpaired electron in an organic radical can be identified through the observation of hyperfine splitting in the EPR spectrum of the radical. The magnitude of this splitting is proportional to the spin density of the unpaired electron at those positions in the radical having atoms with nuclear moments. In addition, the spin density on carbon atoms adjacent to the magnetic nuclei can be determined indirectly through the McConnell relation. Thus, for example, in the benzene negative ion, unpaired spin densities on both the carbon atoms and hydrogen atoms can be determined from the EPR hyperfine splittings. The next step then is to construct a molecular orbital which will theoretically reproduce these experimentally determined spin densities. A good match indicates that we have found a good molecular orbital for the radical.

### Numerical exercises

- E18.4(b)** For  $^{19}\text{F}$   $\frac{\mu}{\mu_N} = 2.62835$ ,  $g = 5.2567$

$$\nu = \nu_L = \frac{\gamma\mathcal{B}}{2\pi} \quad \text{with } \gamma = \frac{gI\mu_N}{\hbar}$$

$$\begin{aligned} \text{Hence, } \nu &= \frac{gI\mu_N\mathcal{B}}{h} = \frac{(5.2567) \times (5.0508 \times 10^{-27} \text{ J T}^{-1}) \times (16.2 \text{ T})}{(6.626 \times 10^{-34} \text{ J s})} \\ &= 6.49 \times 10^8 \text{ s}^{-1} = \boxed{649 \text{ MHz}} \end{aligned}$$

- E18.5(b)**  $E_{m_I} = -\gamma\hbar\mathcal{B}m_I = -gI\mu_N\mathcal{B}m_I$

$$m_I = 1, 0, -1$$

$$\begin{aligned} E_{m_I} &= -(0.404) \times (5.0508 \times 10^{-27} \text{ J T}^{-1}) \times (11.50 \text{ T})m_I \\ &= -(2.3466 \times 10^{-26} \text{ J})m_I \end{aligned}$$

$$\boxed{-2.35 \times 10^{-26} \text{ J}, 0, +2.35 \times 10^{-26} \text{ J}}$$

- E18.6(b)** The energy separation between the two levels is

$$\begin{aligned} \Delta E = h\nu \quad \text{where } \nu &= \frac{\gamma\mathcal{B}}{2\pi} = \frac{(1.93 \times 10^7 \text{ T}^{-1} \text{ s}^{-1}) \times (15.4 \text{ T})}{2\pi} \\ &= 4.73 \times 10^7 \text{ s}^{-1} = \boxed{47.3 \text{ MHz}} \end{aligned}$$

- E18.7(b)** A 600 MHz NMR spectrometer means 600 MHz is the resonance field for protons for which the magnetic field is 14.1 T as shown in Exercise 18.4(a). In high-field NMR it is the field not the frequency that is fixed.

- (a) A  $^{14}\text{N}$  nucleus has three energy states in a magnetic field corresponding to  $m_I = +1, 0, -1$ . But  $\Delta E(+1 \rightarrow 0) = \Delta E(0 \rightarrow -1)$

$$\begin{aligned} \Delta E &= E_{m'_I} - E_{m_I} = -\gamma\hbar\mathcal{B}m'_I - (-\gamma\hbar\mathcal{B}m_I) \\ &= -\gamma\hbar\mathcal{B}(m'_I - m_I) = -\gamma\hbar\mathcal{B}\Delta m_I \end{aligned}$$

The allowed transitions correspond to  $\Delta m_I = \pm 1$ ; hence

$$\begin{aligned} \Delta E = h\nu = \gamma\hbar\mathcal{B} &= gI\mu_N\mathcal{B} = (0.4036) \times (5.051 \times 10^{-27} \text{ J T}^{-1}) \times (14.1 \text{ T}) \\ &= \boxed{2.88 \times 10^{-26} \text{ J}} \end{aligned}$$

- (b) We assume that the electron  $g$ -value in the radical is equal to the free electron  $g$ -value,  $g_e = 2.0023$ . Then

$$\begin{aligned}\Delta E = h\nu &= g_e \mu_B \mathcal{B} [37] = (2.0023) \times (9.274 \times 10^{-24} \text{ J T}^{-1}) \times (0.300 \text{ T}) \\ &= \boxed{5.57 \times 10^{-24} \text{ J}}\end{aligned}$$

**Comment.** The energy level separation for the electron in a free radical in an ESR spectrometer is far greater than that of nuclei in an NMR spectrometer, despite the fact that NMR spectrometers normally operate at much higher magnetic fields.

- E18.8(b)**  $\Delta E = h\nu = \gamma \hbar \mathcal{B} = g_I \mu_N \mathcal{B}$  [Exercise 18.4(a)]

$$\text{Hence, } \mathcal{B} = \frac{h\nu}{g_I \mu_N} = \frac{(6.626 \times 10^{-34} \text{ J Hz}^{-1}) \times (150.0 \times 10^6 \text{ Hz})}{(5.586) \times (5.051 \times 10^{-27} \text{ J T}^{-1})} = \boxed{3.523 \text{ T}}$$

- E18.9(b)** In all cases the selection rule  $\Delta m_I = \pm 1$  is applied; hence (Exercise 18.7(b)(a))

$$\begin{aligned}\mathcal{B} &= \frac{h\nu}{g_I \mu_N} = \frac{6.626 \times 10^{-34} \text{ J Hz}^{-1}}{5.0508 \times 10^{-27} \text{ J T}^{-1}} \times \frac{\nu}{g_I} \\ &= (1.3119 \times 10^{-7}) \times \left(\frac{\nu}{\text{Hz}}\right) \text{ T} = (0.13119) \times \left(\frac{\nu}{\text{MHz}}\right) \text{ T}\end{aligned}$$

We can draw up the following table

$\mathcal{B}/\text{T}$	$^{14}\text{N}$	$^{19}\text{F}$	$^{31}\text{P}$
$g_I$	0.40356	5.2567	2.2634
(a) 300 MHz	97.5	7.49	17.4
(b) 750 MHz	244	18.7	43.5

**Comment.** Magnetic fields above 20 T have not yet been obtained for use in NMR spectrometers. As discussed in the solution to Exercise 18.7(b), it is the field, not the frequency, that is fixed in high-field NMR spectrometers. Thus an NMR spectrometer that is called a 300 MHz spectrometer refers to the resonance frequency for protons and has a magnetic field fixed at 7.05 T.

- E18.10(b)** The relative population difference for spin  $-\frac{1}{2}$  nuclei is given by

$$\begin{aligned}\frac{\delta N}{N} &= \frac{N_\alpha - N_\beta}{N_\alpha + N_\beta} \approx \frac{\gamma \hbar \mathcal{B}}{2kT} = \frac{g_I \mu_N \mathcal{B}}{2kT} \quad [\textit{Justification 18.1}] \\ &= \frac{1.405(5.05 \times 10^{-27} \text{ J T}^{-1}) \mathcal{B}}{2(1.381 \times 10^{-23} \text{ J K}^{-1}) \times (298 \text{ K})} = 8.62 \times 10^{-7} (\mathcal{B}/\text{T})\end{aligned}$$

(a) For 0.50 T  $\frac{\delta N}{N} = (8.62 \times 10^{-7}) \times (0.50) = \boxed{4.3 \times 10^{-7}}$

(b) For 2.5 T  $\frac{\delta N}{N} = (8.62 \times 10^{-7}) \times (2.5) = \boxed{2.2 \times 10^{-6}}$

(c) For 15.5 T  $\frac{\delta N}{N} = (8.62 \times 10^{-7}) \times (15.5) = \boxed{1.34 \times 10^{-5}}$

**E18.11(b)** The ground state has

$$m_I = +\frac{1}{2} = \alpha \text{ spin}, \quad m_I = -\frac{1}{2} = \beta \text{ spin}$$

Hence, with

$$\begin{aligned} \delta N &= N_\alpha - N_\beta \\ \frac{\delta N}{N} &= \frac{N_\alpha - N_\beta}{N_\alpha + N_\beta} = \frac{N_\alpha - N_\alpha e^{-\Delta E/kT}}{N_\alpha + N_\alpha e^{-\Delta E/kT}} \quad [\text{Justification 18.1}] \\ &= \frac{1 - e^{-\Delta E/kT}}{1 + e^{-\Delta E/kT}} \approx \frac{1 - (1 - \Delta E/kT)}{1 + 1} \approx \frac{\Delta E}{2kT} = \frac{g_I \mu_N \mathcal{B}}{2kT} \quad [\text{for } \Delta E \ll kT] \\ \delta N &= \frac{Ng_I \mu_N \mathcal{B}}{2kT} = \frac{Nh\nu}{2kT} \end{aligned}$$

Thus,  $\delta N \propto \nu$

$$\frac{\delta N(800 \text{ MHz})}{\delta N(60 \text{ MHz})} = \frac{800 \text{ MHz}}{60 \text{ MHz}} = \boxed{13}$$

This ratio is not dependent on the nuclide as long as the approximation  $\Delta E \ll kT$  holds.

(a)  $\delta = \frac{\nu - \nu^\circ}{\nu^\circ} \times 10^6$  [18.25]

Since both  $\nu$  and  $\nu^\circ$  depend upon the magnetic field in the same manner, namely

$$\nu = \frac{g_I \mu_N \mathcal{B}}{h} \quad \text{and} \quad \nu^\circ = \frac{g_I \mu_N \mathcal{B}_0}{h} \quad [\text{Exercise 18.4(a)}]$$

$\delta$  is independent of both  $\mathcal{B}$  and  $\nu$ .

(b) Rearranging [10]  $\nu - \nu^\circ = \nu^\circ \delta \times 10^{-6}$   
and we see that the relative chemical shift is

$$\frac{\nu - \nu^\circ(800 \text{ MHz})}{\nu - \nu^\circ(60 \text{ MHz})} = \frac{800 \text{ MHz}}{60 \text{ MHz}} = \boxed{13}$$

**Comment.** This direct proportionality between  $\nu - \nu^\circ$  and  $\nu^\circ$  is one of the major reasons for operating an NMR spectrometer at the highest frequencies possible.

**E18.12(b)**  $\mathcal{B}_{\text{loc}} = (1 - \sigma)\mathcal{B}$

$$\begin{aligned} |\Delta \mathcal{B}_{\text{loc}}| &= |(\Delta \sigma)|\mathcal{B} \approx |[\delta(\text{CH}_3) - \delta(\text{CH}_2)]|\mathcal{B} \\ &= |1.16 - 3.36| \times 10^{-6} \mathcal{B} = 2.20 \times 10^{-6} \mathcal{B} \end{aligned}$$

(a)  $\mathcal{B} = 1.9 \text{ T}$ ,  $|\Delta \mathcal{B}_{\text{loc}}| = (2.20 \times 10^{-6}) \times (1.9 \text{ T}) = \boxed{4.2 \times 10^{-6} \text{ T}}$

(b)  $\mathcal{B} = 16.5 \text{ T}$ ,  $|\Delta \mathcal{B}_{\text{loc}}| = (2.20 \times 10^{-6}) \times (16.5 \text{ T}) = \boxed{3.63 \times 10^{-5} \text{ T}}$

**E18.13(b)**  $\nu - \nu^\circ = \nu^\circ \delta \times 10^{-6}$

$$\begin{aligned} |\Delta \nu| &\equiv (\nu - \nu^\circ)(\text{CH}_2) - (\nu - \nu^\circ)(\text{CH}_3) = \nu(\text{CH}_2) - \nu(\text{CH}_3) \\ &= \nu^\circ [\delta(\text{CH}_2) - \delta(\text{CH}_3)] \times 10^{-6} \\ &= (3.36 - 1.16) \times 10^{-6} \nu^\circ = 2.20 \times 10^{-6} \nu^\circ \end{aligned}$$

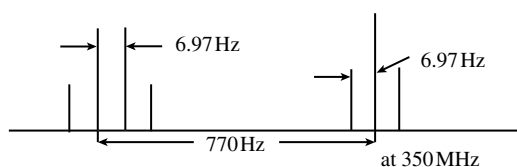


Figure 18.1

- (a)  $\nu^\circ = 350 \text{ MHz}$   $|\Delta\nu| = (2.20 \times 10^{-6}) \times (350 \text{ MHz}) = 770 \text{ Hz}$  [Fig. 18.1]  
 (b)  $\nu^\circ = 650 \text{ MHz}$   $|\Delta\nu| = (2.20 \times 10^{-6}) \times (650 \text{ MHz}) = 1.43 \text{ kHz}$

At 650 MHz, the spin-spin splitting remains the same at 6.97 Hz, but as  $\Delta\nu$  has increased to 1.43 kHz, the splitting appears narrower on the  $\delta$  scale.

**E18.14(b)** The difference in resonance frequencies is

$$\Delta\nu = (\nu^\circ \times 10^{-6})\Delta\delta = (350 \text{ s}^{-1}) \times (6.8 - 5.5) = 4.6 \times 10^2 \text{ s}^{-1}$$

The signals will be resolvable as long as the conformations have lifetimes greater than

$$\tau = (2\pi \Delta\delta)^{-1}$$

The interconversion rate is the reciprocal of the lifetime, so a resolvable signal requires an interconversion rate less than

$$\text{rate} = (2\pi \Delta\delta) = 2\pi(4.6 \times 10^2 \text{ s}^{-1}) = \boxed{2.9 \times 10^3 \text{ s}^{-1}}$$

**E18.15(b)**  $\nu = \frac{gI\mu_N B}{h}$  [Exercise 18.4(a)]

$$\text{Hence, } \frac{\nu(^{31}\text{P})}{\nu(^1\text{H})} = \frac{g(^{31}\text{P})}{g(^1\text{H})}$$

$$\text{or } \nu(^{31}\text{P}) = \frac{2.2634}{5.5857} \times 500 \text{ MHz} = \boxed{203 \text{ MHz}}$$

The proton resonance consists of 2 lines ( $2 \times \frac{1}{2} + 1$ ) and the  $^{31}\text{P}$  resonance of 5 lines [ $2 \times (4 \times \frac{1}{2}) + 1$ ]. The intensities are in the ratio 1:4:6:4:1 (Pascal's triangle for four equivalent spin  $\frac{1}{2}$  nuclei, Section 18.6). The lines are spaced  $\frac{5.5857}{2.2634} = 2.47$  times greater in the phosphorus region than the proton region. The spectrum is sketched in Fig. 18.2.

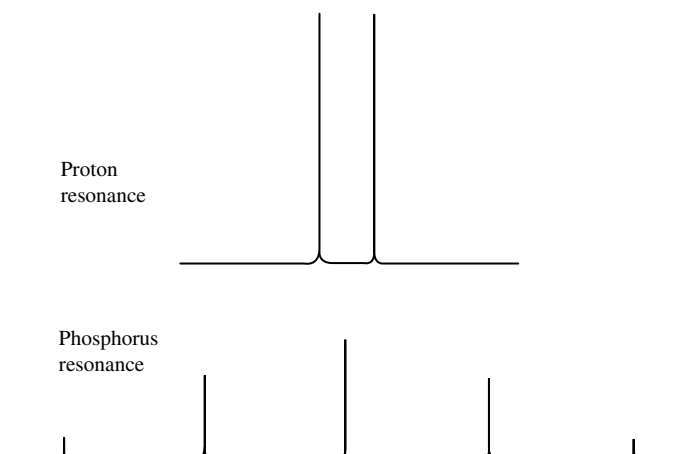


Figure 18.2

**E18.16(b)** Look first at A and M, since they have the largest splitting. The A resonance will be split into a widely spaced triplet (by the two M protons); each peak of that triplet will be split into a less widely spaced sextet (by the five X protons). The M resonance will be split into a widely spaced triplet (by the two A protons); each peak of that triplet will be split into a narrowly spaced sextet (by the five X protons). The X resonance will be split into a less widely spaced triplet (by the two A protons); each peak of that triplet will be split into a narrowly spaced triplet (by the two M protons). (See Fig. 18.3.)

Only the splitting of the central peak of Fig. 18.3(a) is shown in Fig. 18.3(b).

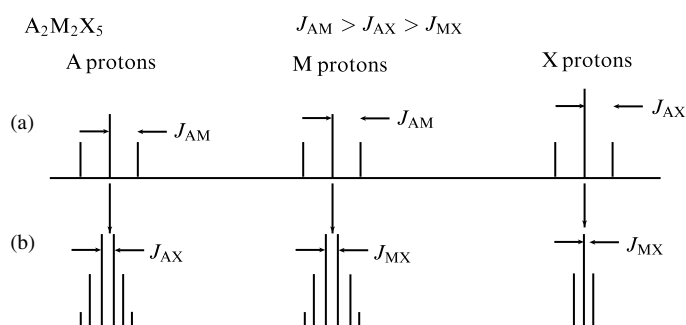


Figure 18.3

- E18.17(b)** (a) Since all  $J_{HF}$  are equal in this molecule (the  $CH_2$  group is perpendicular to the  $CF_2$  group), the H and F nuclei are both chemically and magnetically equivalent.  
 (b) Rapid rotation of the  $PH_3$  groups about the Mo–P axes makes the P and H nuclei chemically and magnetically equivalent in both the *cis*- and *trans*-forms.

**E18.18(b)** Precession in the rotating frame follows

$$\nu_L = \frac{\gamma B_1}{2\pi} \quad \text{or} \quad \omega_1 = \gamma B_1$$

Since  $\omega$  is an angular frequency, the angle through which the magnetization vector rotates is

$$\theta = \gamma B_1 t = \frac{gI\mu_N}{\hbar} B_1 t$$

$$\text{So } B_1 = \frac{\theta \hbar}{gI\mu_N t} = \frac{(\pi) \times (1.0546 \times 10^{-34} \text{ J s})}{(5.586) \times (5.0508 \times 10^{-27} \text{ J T}^{-1}) \times (12.5 \times 10^{-6} \text{ s})} = \boxed{9.40 \times 10^{-4} \text{ T}}$$

$$\text{a } 90^\circ \text{ pulse requires } \frac{1}{2} \times 12.5 \mu\text{s} = \boxed{6.25 \mu\text{s}}$$

**E18.19(b)** 
$$B = \frac{h\nu}{g_e\mu_B} = \frac{hc}{g_e\mu_B\lambda}$$

$$= \frac{(6.626 \times 10^{-34} \text{ J s}) \times (2.998 \times 10^8 \text{ m s}^{-1})}{(2) \times (9.274 \times 10^{-24} \text{ J T}^{-1}) \times (8 \times 10^{-3} \text{ m})} = \boxed{1.3 \text{ T}}$$

**E18.20(b)** The  $g$  factor is given by

$$g = \frac{h\nu}{\mu_B B}; \quad \frac{h}{\mu_B} = \frac{6.62608 \times 10^{-34} \text{ J s}}{9.2740 \times 10^{-24} \text{ J T}^{-1}} = 7.1448 \times 10^{-11} \text{ T Hz}^{-1} = 71.448 \text{ mT GHz}^{-1}$$

$$g = \frac{71.448 \text{ mT GHz}^{-1} \times 9.2482 \text{ GHz}}{330.02 \text{ mT}} = \boxed{2.0022}$$

**E18.21(b)** The hyperfine coupling constant for each proton is  $2.2 \text{ mT}$ , the difference between adjacent lines in the spectrum. The  $g$  value is given by

$$g = \frac{h\nu}{\mu_B B} = \frac{(71.448 \text{ mT GHz}^{-1}) \times (9.332 \text{ GHz})}{334.7 \text{ mT}} = 1.992$$

**E18.22(b)** If the spectrometer has sufficient resolution, it will see a signal split into eight equal parts at  $\pm 1.445 \pm 1.435 \pm 1.055 \text{ mT}$  from the centre, namely

$$328.865, 330.975, 331.735, 331.755, 333.845, 333.865, 334.625, \text{ and } 336.735 \text{ mT}$$

If the spectrometer can only resolve to the nearest  $0.1 \text{ mT}$ , then the spectrum will appear as a sextet with intensity ratios of  $1 : 1 : 2 : 2 : 1 : 1$ . The four central peaks of the more highly resolved spectrum would be the two central peaks of the less resolved spectrum.

**E18.23(b)** (a) If the  $\text{CH}_2$  protons have the larger splitting there will be a triplet ( $1 : 2 : 1$ ) of quartets ( $1 : 3 : 3 : 1$ ). Altogether there will be 12 lines with relative intensities 1(4 lines), 2(2 lines), 3(4 lines), and 6(2 lines). Their positions in the spectrum will be determined by the magnitudes of the two proton splittings which are not given.

(b) If the  $\text{CD}_2$  deuterons have the larger splitting there will be a quintet ( $1 : 2 : 3 : 2 : 1$ ) of septets ( $1 : 3 : 6 : 7 : 6 : 3 : 1$ ). Altogether there will be 35 lines with relative intensities 1(4 lines), 2(4 lines), 3(6 lines), 6(8 lines), 7(2 lines), 9(2 lines), 12(4 lines), 14(2 lines), 18(2 lines), and 21(1 line). Their positions in the spectrum will be determined by the magnitude of the two deuteron splittings which are not given.

**E18.24(b)** The hyperfine coupling constant for each proton is  $2.2 \text{ mT}$ , the difference between adjacent lines in the spectrum. The  $g$  value is given by

$$g = \frac{h\nu}{\mu_B B} \quad \text{so} \quad B = \frac{h\nu}{\mu_B g}, \quad \frac{h}{\mu_B} = 71.448 \text{ mT GHz}^{-1}$$

$$(a) \quad B = \frac{(71.448 \text{ mT GHz}^{-1}) \times (9.312 \text{ GHz})}{2.0024} = 332.3 \text{ mT}$$

$$(b) \quad B = \frac{(71.448 \text{ mT GHz}^{-1}) \times (33.88 \text{ GHz})}{2.0024} = 1209 \text{ mT}$$

**E18.25(b)** Two nuclei of spin  $I = 1$  give five lines in the intensity ratio  $1 : 2 : 3 : 2 : 1$  (Fig. 18.4).

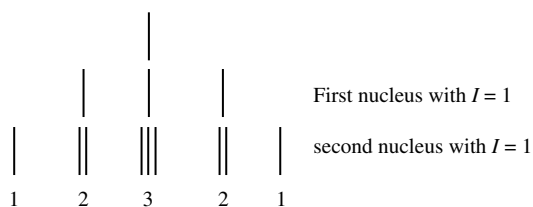


**Figure 18.4**

**E18.26(b)** The X nucleus produces four lines of equal intensity. The three H nuclei split each into a  $1 : 3 : 3 : 1$  quartet. The three D nuclei split each line into a septet with relative intensities  $1 : 3 : 6 : 7 : 6 : 3 : 1$  (see Exercise 18.23(a)). (See Fig. 18.5.)

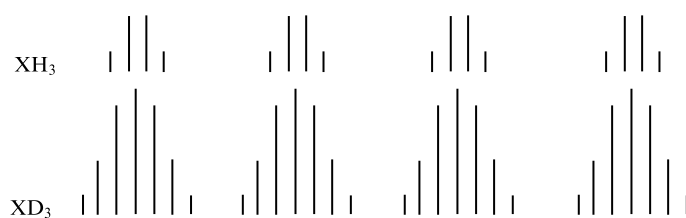


Figure 18.5

## Solutions to problems

### Solutions to numerical problems

**P18.2**

$$\tau_J \approx \frac{1}{2\pi\delta\nu} = \frac{1}{(2\pi) \times ((5.2 - 4.0) \times 10^{-6}) \times (60 \times 10^6 \text{ Hz})}$$

$$\approx 2.2 \text{ ms, corresponding to a rate of jumping of } 450 \text{ s}^{-1}.$$

When  $\nu = 300 \text{ MHz}$

$$\tau_J \approx \frac{1}{(2\pi) \times \{(5.2 - 4.0) \times 10^{-6}\} \times (300 \times 10^6 \text{ Hz})} = 0.44 \text{ ms}$$

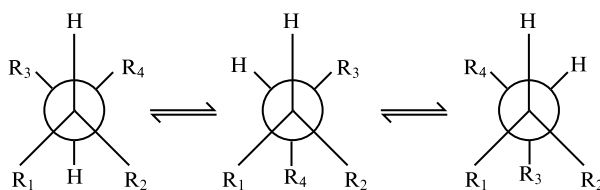
corresponding to a jump rate of  $2.3 \times 10^3 \text{ s}^{-1}$ . Assume an Arrhenius-like jumping process (Chapter 25)

$$\text{rate} \propto e^{-E_a/RT}$$

$$\text{Then, } \ln \left[ \frac{\text{rate}(T')}{\text{rate}(T)} \right] = \frac{-E_a}{R} \left( \frac{1}{T'} - \frac{1}{T} \right)$$

$$\text{and therefore } E_a = \frac{R \ln(r'/r)}{\frac{1}{T} - \frac{1}{T'}} = \frac{8.314 \text{ J K}^{-1} \text{ mol}^{-1} \times \ln \frac{2.3 \times 10^3}{450}}{\frac{1}{280 \text{ K}} - \frac{1}{300 \text{ K}}} = \boxed{57 \text{ kJ mol}^{-1}}$$

**P18.5** It seems reasonable to assume that only staggered conformations can occur. Therefore the equilibria are



When  $R_3 = R_4 = \text{H}$ , all three of the above conformations occur with equal probability; hence

$${}^3J_{\text{HH}}(\text{methyl}) = \frac{1}{3} ({}^3J_t + 2{}^3J_g) \quad [\text{t} = \text{trans, g} = \text{gauche; CHR}_3\text{R}_4 = \text{methyl}]$$

Additional methyl groups will avoid being staggered between both  $R_1$  and  $R_2$ . Therefore

$${}^3J_{\text{HH}}(\text{ethyl}) = \frac{1}{2} (J_t + J_g) \quad [\text{R}_3 = \text{H, R}_4 = \text{CH}_3]$$

$${}^3J_{\text{HH}}(\text{isopropyl}) = J_t \quad [\text{R}_3 = \text{R}_4 = \text{CH}_3]$$



We then have three simultaneous equations in two unknowns  $J_t$  and  $J_g$ .

$$\frac{1}{3}(^3J_t + 2^3J_g) = 7.3 \text{ Hz} \quad (1)$$

$$\frac{1}{2}(^3J_t + ^3J_g) = 8.0 \text{ Hz} \quad (2)$$

$$^3J_t = 11.2 \text{ Hz}$$

The two unknowns are overdetermined. The first two equations yield  $^3J_t = 10.1$ ,  $^3J_g = 5.9$ . However, if we assume that  $^3J_t = 11.2$  as measured directly in the ethyl case then  $^3J_g = 5.4$  (eqn 1) or 4.8 (eqn 2), with an average value of 5.1.

Using the original form of the Karplus equation

$$^3J_t = A \cos^2(180^\circ) + B = 11.2$$

$$^3J_g = A \cos^2(60^\circ) + B = 5.1$$

or

$$11.2 = A + B$$

$$5.1 = 0.25A + B$$

These simultaneous equations yield  $A = 6.8 \text{ Hz}$  and  $B = 4.8 \text{ Hz}$ . With these values of  $A$  and  $B$ , the original form of the Karplus equation fits the data exactly (at least to within the error in the values of  $^3J_t$  and  $^3J_g$  and in the measured values reported).

From the form of the Karplus equation in the text [21] we see that those values of  $A$ ,  $B$ , and  $C$  cannot be determined from the data given, as there are three constants to be determined from only two values of  $J$ . However, if we use the values of  $A$ ,  $B$ , and  $C$  given in the text, then

$$J_t = 7 \text{ Hz} - 1 \text{ Hz}(\cos 180^\circ) + 5 \text{ Hz}(\cos 360^\circ) = 11 \text{ Hz}$$

$$J_g = 7 \text{ Hz} - 1 \text{ Hz}(\cos 60^\circ) + 5 \text{ Hz}(\cos 120^\circ) = 5 \text{ Hz}$$

The agreement with the modern form of the Karplus equation is excellent, but not better than the original version. Both fit the data equally well. But the modern version is preferred as it is more generally applicable.

**P18.8** Refer to the figure in the solution to Exercise 18.23(a). The width of the  $\text{CH}_3$  spectrum is  $3a_{\text{H}} = 6.9 \text{ mT}$ . The width of the  $\text{CD}_3$  spectrum is  $6a_{\text{D}}$ . It seems reasonable to assume, since the hyperfine interaction is an interaction of the magnetic moments of the nuclei with the magnetic moment of the electron, that the strength of the interactions is proportional to the nuclear moments.

$$\mu = g_I \mu_{\text{N}} I \quad \text{or} \quad \mu_z = g_I \mu_{\text{N}} m_I \quad [18.14, 18.15]$$

and thus nuclear magnetic moments are proportional to the nuclear  $g$ -values; hence

$$a_{\text{D}} \approx \frac{0.85745}{5.5857} \times a_{\text{H}} = 0.1535 a_{\text{H}} = 0.35 \text{ mT}$$

Therefore, the overall width is  $6a_{\text{D}} = 2.1 \text{ mT}$

**P18.10** We write  $P(\text{N}2s) = \frac{5.7 \text{ mT}}{55.2 \text{ mT}} = 0.10$  (10 percent of its time)

$$P(\text{N}2p_z) = \frac{1.3 \text{ mT}}{3.4 \text{ mT}} = 0.38 \quad (38 \text{ percent of its time})$$

The total probability is

(a)  $P(N) = 0.10 + 0.38 = \boxed{0.48}$  (48 percent of its time).

(b)  $P(O) = 1 - P(N) = \boxed{0.52}$  (52 percent of its time).

The hybridization ratio is

$$\frac{P(N2p)}{P(B2s)} = \frac{0.38}{0.10} = \boxed{3.8}$$

The unpaired electron therefore occupies an orbital that resembles as  $sp^3$  hybrid on N, in accord with the radical's nonlinear shape.

From the discussion in Section 14.3 we can write

$$a^2 = \frac{1 + \cos \Phi}{1 - \cos \Phi}$$

$$b^2 = 1 - a^2 = \frac{-2 \cos \Phi}{1 - \cos \Phi}$$

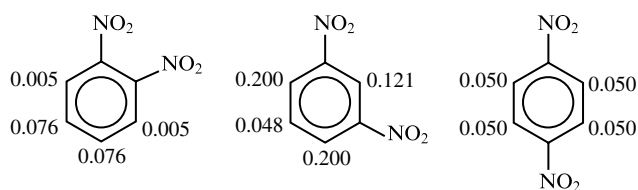
$$\lambda = \frac{b'^2}{a'^2} = \frac{-1 \cos \Phi}{1 + \cos \Phi}, \text{ implying that } \cos \Phi = \frac{\lambda}{2 + \ell}$$

Then, since  $\lambda = 3.8$ ,  $\cos \Phi = -0.66$ , so  $\Phi = \boxed{131^\circ}$

**P18.11** For  $C_6H_6^-$ ,  $a = Q\rho$  with  $Q = 2.25 \text{ mT}$  [18.52]. If we assume that the value of  $Q$  does not change from this value (a good assumption in view of the similarity of the anions), we may write

$$\rho = \frac{a}{Q} = \frac{a}{2.25 \text{ mT}}$$

Hence, we can construct the following maps



### Solutions to theoretical problems

**P18.14**  $\mathcal{B}_{\text{nuc}} = -\frac{\gamma \hbar \mu_0 m_I}{4\pi R^3} (1 - 3 \cos^2 \theta)$  [18.36] =  $\frac{g_I \mu_N \mu_0}{4\pi R^3} [m_I = +\frac{1}{2}, \theta = 0, \gamma \hbar = g_I \mu_N]$

which rearranges to

$$R = \left( \frac{g_I \mu_N \mu_0}{4\pi \mathcal{B}_{\text{nuc}}} \right)^{1/3} = \left( \frac{(5.5857) \times (5.0508 \times 10^{-27} \text{ JT}^{-1}) \times (4\pi \times 10^{-7} \text{ T}^2 \text{ J}^{-1} \text{ m}^3)}{(4\pi) \times (0.715 \times 10^{-3} \text{ T})} \right)^{1/3}$$

$$= (3.946 \times 10^{-30} \text{ m}^3)^{1/3} = \boxed{158 \text{ pm}}$$

**P18.17** We have seen (Problem 18.16) that, if  $G \propto \cos \omega_0 t$ , then  $I(\omega) \propto \frac{1}{[1 + (\omega_0 - \omega)^2 \tau^2]}$  which peaks at  $\omega \approx \omega_0$ . Therefore, if

$$G(t) \propto a \cos \omega_1 t + b \cos \omega_2 t$$

we can anticipate that

$$I(\omega) \propto \frac{a}{1 + (\omega_1 - \omega)^2 \tau^2} + \frac{b}{1 + (\omega_2 - \omega)^2 \tau^2}$$

and explicit calculation shows this to be so. Therefore,  $I(\omega)$  consists of two absorption lines, one peaking at  $\omega \approx \omega_1$  and the other at  $\omega \approx \omega_2$ .

**P18.21** The desired result is the linear equation:

$$[I]_0 = \frac{[E]_0 \Delta \nu}{\delta \nu} - K,$$

so the first task is to express quantities in terms of  $[I]_0$ ,  $[E]_0$ ,  $\Delta \nu$ ,  $\delta \nu$ , and  $K$ , eliminating terms such as  $[I]$ ,  $[EI]$ ,  $[E]$ ,  $\nu_I$ ,  $\nu_{EI}$ , and  $\nu$ . (Note: symbolic mathematical software is helpful here.) Begin with  $\nu$ :

$$\nu = \frac{[I]}{[I] + [EI]} \nu_I + \frac{[EI]}{[I] + [EI]} \nu_{EI} = \frac{[I]_0 - [EI]}{[I]_0} \nu_I + \frac{[EI]}{[I]_0} \nu_{EI},$$

where we have used the fact that total I (*i.e.*, free I plus bound I) is the same as initial I. Solve this expression for  $[EI]$ :

$$[EI] = \frac{[I]_0(\nu - \nu_I)}{\nu_{EI} - \nu_I} = \frac{[I]_0 \delta \nu}{\Delta \nu},$$

where in the second equality we notice that the frequency differences that appear are the ones defined in the problem. Now take the equilibrium constant:

$$K = \frac{[E][I]}{[EI]} = \frac{([E]_0 - [EI])([I]_0 - [EI])}{[EI]} \approx \frac{([E]_0 - [EI])[I]_0}{[EI]}.$$

We have used the fact that total I is much greater than total E (from the condition that  $[I]_0 \gg [E]_0$ ), so it must also be much greater than  $[EI]$ , even if all E binds I. Now solve this for  $[E]_0$ :

$$[E]_0 = \frac{K + [I]_0}{[I]_0} [EI] = \left( \frac{K + [I]_0}{[I]_0} \right) \left( \frac{[I]_0 \delta \nu}{\Delta \nu} \right) = \frac{(K + [I]_0) \delta \nu}{\Delta \nu}.$$

The expression contains the desired terms and only those terms. Solving for  $[I]_0$  yields:

$$\boxed{[I]_0 = \frac{[E]_0 \Delta \nu}{\delta \nu} - K},$$

which would result in a straight line with slope  $[E]_0 \Delta \nu$  and  $y$ -intercept  $K$  if one plots  $[I]_0$  against  $1/\delta \nu$ .